

Electronic Supplementary Information

Novel near-infrared theranostic probe for accurate cancer chemotherapy in vivo by dual activation strategy

Wen-Xin Wang,^a Wen-Li Jiang,^a Guo-Jiang Mao,^{*,b} Zhi-Ke Tan,^a Min Tan,^a and Chun-Yan Li^{*,a}

^a Key Laboratory for Green Organic Synthesis and Application of Hunan Province, Key Laboratory of Environmentally Friendly Chemistry and Applications of Ministry of Education, College of Chemistry, Xiangtan University, Xiangtan, 411105, PR China.

^b Henan Key Laboratory of Organic Functional Molecule and Drug Innovation, Collaborative Innovation Center of Henan Province for Green Manufacturing of Fine Chemicals, Key Laboratory of Green Chemical Media and Reactions, Ministry of Education, School of Chemistry and Chemical Engineering, Henan Normal University, Xinxiang, 453007, PR China.

*Corresponding Author. E-mail: lichunyan79@sina.com; maoguojiang@htu.edu.cn

Table of contents

1. Experimental Section.....	S3
2. Synthesis of probes.....	S6
3. Spectral data.....	S14
4. Response mechanism.....	S15
5. Biological assays.....	S18

1. Experimental Section.

Reagents and instruments. Cyclohexanone, phosphorus tribromide (PBr₃), 2-hydroxy-4-methoxybenzaldehyde, cesium carbonate (Cs₂CO₃), boron tribromide (BBr₃), 4-(diethylamino) salicylaldehyde, ethyl acetoacetate, piperidine, 4-(bromomethyl) benzene boronic acid, 5'-deoxy-5-fluorouridine (5'-DFUR) were purchased from Aladdin (Shanghai, China). Nuclear magnetic resonance (NMR) spectra were measured on a Bruker Avance II NMR spectrometer (Germany). Mass spectra (MS) was acquired on a Bruker Autoflex MALDI-TOF mass spectrometer (Germany). HPLC was carried out on a Agilent 1260 LC system with a C18 column (USA). Element analysis was conducted on Perkin Elmer 2400 elemental analyzer (USA).

General Procedure for Fluorescence Detection. The stock solution of CX-B-DF was obtained in DMSO. The stock solution of H₂O₂ was obtained by diluting H₂O₂ (30%) with deionized water. The test solution was prepared with PBS buffer solution (50 mM, pH 7.4) in a 4 mL quartz cuvette. The final concentration CX-B-DF were 1.0×10^{-5} M and H₂O₂ were 8.0×10^{-5} - 1.0×10^{-6} M. The fluorescence spectra were obtained on a Hitachi F-4600 spectrophotometer (Japan) with the excitation at 550 nm, and the emission at 585-850 nm

Cell culture and imaging. The 293T cells, HCT116 cells and 4T1 cells were provided by the State Key Laboratory of Chemo/Biosensing and Chemometrics of Hunan University (Changsha, China). The cells were cultured in DMEM (Dulbecco's modified Eagle's medium) containing 1% antibiotics (100 U/mL penicillin and 100 µg/mL streptomycin) and 10 % FBS (fetal bovine serum) in an atmosphere of 37 °C and 5% CO₂. When the cell density reached 90% of confluence, a subculture was done and the medium was changed approximately every

day. The cells were seeded in a 20 mm glass-bottom dish plated and grown to around 80% confluency for 24 h before the experiment.

The cells were divided into two groups. One group was treated with CX-B-DF (10 μ M) at 37 °C for 0 h, 0.5 h, 1 h and 2 h, respectively. The other group was pretreated with H₂O₂ (50 μ M) for 30 min, then treated with CX-B-DF (10 μ M) at 37 °C for 30 min. All the cells were washed by PBS buffer solution three times and fluorescence image of cells were performed by a Nikon confocal fluorescence microscope (Japan).

Cell Cytotoxicity Assay. The cytotoxicity of the compounds was evaluated by CCK-8 and AO/DAPI counterstaining assay, respectively. CCK-8 assay measures the activity of mitochondria in living cells, and was done by using commercial kits purchased from Beyotime (Nantong, China). AO/DAPI staining was done by using commercial kits (solution 13) purchased from ChemoMetec A/S (Allerod, Denmark). In this assay, all the cells were stained with green fluorescence by AO, whereas dead cells were stained with blue fluorescence by DAPI. The stained cells were imaged and the cell viability was calculated by NucleoCounter NC-3000 (ChemoMetec A/S, Allerod, Denmark).

Fluorescence Imaging of H₂O₂ in Tumor-bearing Mice. Six week-old male BALB/C nude mice were chosen and kindly kept in all the experimental process. The mice were underarm injected with HCT116 cells to establish tumor model. All experiments were performed in accordance with “Regulations of Hunan province on the administration of experimental animals”.

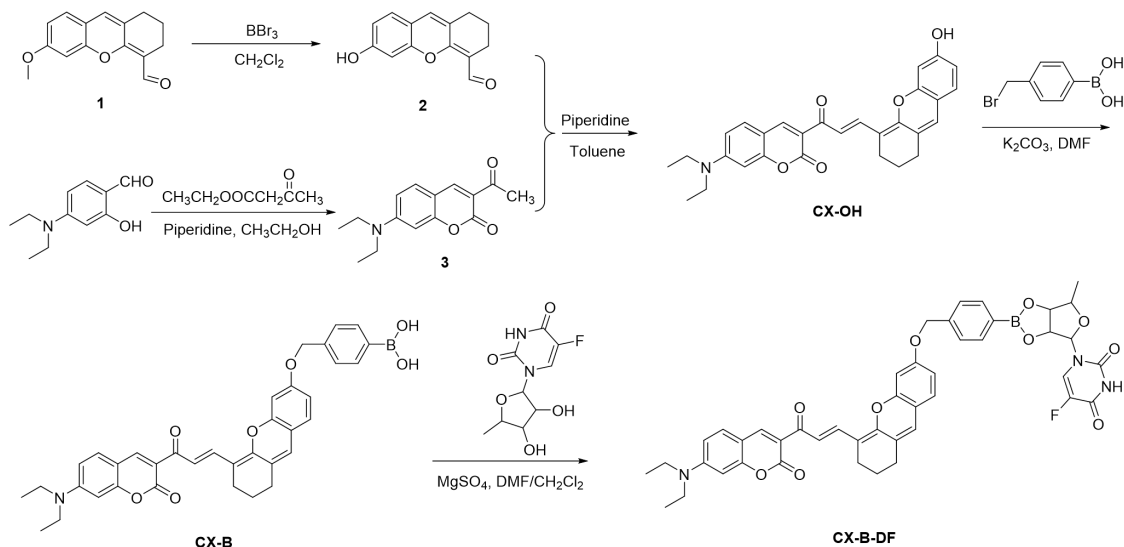
Before imaging, the mice were fasted for 12 h to avoid possible food fluorescence interference. The tumor-bearing mice were divided into three groups and treated differently.

The first group of mice was intratumorally injected with CX-B-DF (200 μ M in 100 μ L PBS). The second group was intravenously injected with PBS (100 μ L). The third group was intravenously injected with CX-B-DF (200 μ M in 100 μ L PBS). Then, the fluorescence images were acquired with an IVIS Lumina XR small animal optical in vivo imaging system (USA). The mice were anesthetized with isoflurane and remained anesthetized throughout the image period.

For ex-vivo imaging, the above mice were sacrificed and major organs including heart, liver, spleen, lung, kidneys and tumors were excised, washed with PBS solution and imaged.

In Vivo Antitumor Studies. HCT116 cells (1×10^6) were injected into the armpits of the nude mice, all of which developed tumors in 7 d with sizes of 50 mm³ by average. The mice were randomly assigned into 3 groups (3 mice/group), and treated by CX-B-DF, CX-B and PBS (control group) at a dose of 10 mg/kg by intravenous injection every 3 days for 5 times, respectively. After 22 days of treatment, the weight of tumors in each group of mice was recorded. To evaluate the effect of treatment, inhibition rates (IRT) of tumor growth were calculated according to the equation: $IRT = 100\% \times (\text{mean tumor weight of control group} - \text{mean tumor weight of experimental group}) / \text{mean tumor weight of control group}$.

2. Synthesis of CX-B-DF.



Scheme S1. Synthetic route for CX-B-DF.

Compound 2. Compound **1** was synthesized according to our previous report (Sens Actuators B Chem., 2020, 320, 128296). At 0 °C, compound **1** (0.24 g, 1.0 mmol) was dissolved in dry CH_2Cl_2 (5 mL), and BBr_3 (1.25 g, 5.0 mmol) was slowly dripped under stirring. Then, it was continued to react at room temperature for 16 h. Subsequently, the reaction was quenched by adding saturated NaHCO_3 solution under ice bath. And the solution was extracted with $\text{CH}_2\text{Cl}_2/\text{CH}_3\text{OH}$ (20:1). The organic layer was dried by anhydrous Na_2SO_4 and then the solvent was removed. The crude product was purified by column chromatography ($\text{CH}_2\text{Cl}_2:\text{CH}_3\text{OH} = 50:1$) to afford an orange solid. Yield: 0.19 g (83%). ^1H NMR (400 MHz, CDCl_3) δ 10.04 (s, 1H), 7.02 (d, $J = 8.9$ Hz, 1H), 6.73 (s, 1H), 6.56 (d, $J = 5.2$ Hz, 2H), 2.51 (t, $J = 5.9$ Hz, 2H), 2.33 (t, $J = 5.9$ Hz, 2H), 1.67-1.62 (m, 2H). MS (TOF): 228.4.

Compound 3. 4-(Diethylamino) salicylaldehyde (0.49 g, 2.5 mmol), acetylacetic ether (0.33 g, 2.5 mmol), and piperidine (0.1 mL) were dissolved in ethanol. The mixture was

refluxed for 6 h and HCl (4 M, 10 mL) was poured into the solution stirred at 60 °C for 0.5 h. The mixture was extracted with ethyl acetate and the organic layer was dried with anhydrous Na₂SO₄. The crude product was subjected to silica gel chromatography with CH₂Cl₂ as eluent to give yellow solid. Yield: 0.42 g (65%). ¹H NMR (400 MHz, CDCl₃) δ 8.44 (s, 1H), 7.41 (d, J = 9.0 Hz, 1H), 6.66 - 6.63 (m, 1H), 6.49 (d, J = 2.1 Hz, 1H), 3.46 (q, J = 7.1 Hz, 4H), 2.68 (s, 3H), 1.25 (t, J = 7.1 Hz, 6H). MS (TOF): 260.3.

Compound CX-OH. Compound **2** (0.23 g, 1.0 mmol), compound **3** (0.26 g, 1.0 mmol) and piperidine (0.2 mL) were dissolved in toluene (10 mL). Next, the mixture was refluxed for 12 h. The solution was concentrated and the crude product was purified by column chromatography (CH₂Cl₂:CH₃OH = 30:1) to afford a brown solid. Yield: 0.24 g (51%). ¹H NMR (400 MHz, DMSO-d₆) δ 10.11 (s, 1H), 8.54 (s, 1H), 8.09 (d, J = 16.0 Hz, 1H), 7.67 (d, J = 8.0 Hz, 1H), 7.32 (d, J = 16.0 Hz, 1H), 7.09 (d, J = 8.0 Hz, 1H), 6.80-6.77 (m, 1H), 6.68 (s, 1H), 6.58 (s, 1H), 6.53-6.50 (m, 2H), 3.51-3.46 (m, 4H), 2.41 (t, J = 4.0 Hz, 4H), 1.74-1.68 (m, 2H), 1.14 (t, J = 4.0 Hz, 6H). ¹³C NMR (100 MHz, DMSO-d₆) δ 184.9, 160.6, 159.7, 158.4, 154.0, 153.2, 148.1, 137.3, 132.6, 128.0, 126.5, 125.0, 120.3, 116.8, 114.0, 110.5, 110.1, 108.5, 102.0, 96.4, 45.0, 29.4, 25.0, 20.9, 13.0. MS (TOF): 470.4.

Compound CX-B. Under N₂ atmosphere, **CX-OH** (117 mg, 0.25 mmol), 4-(bromomethyl) benzenboronic acid (106 mg, 0.5 mmol) and K₂CO₃ (68 mg, 0.5 mmol) were dissolved in DMF (7 mL). The mixture was stirred at 60 °C for 6 h. Then, the solvent was removed and the obtained crude product was further purified by silica gel column chromatography (CH₂Cl₂:CH₃OH = 20:1) to afford a blue solid. Yield: 60 mg (40%). ¹H NMR (400 MHz, DMSO-d₆) δ 8.53 (s, 1H), 8.13-8.07 (m, 2H), 7.81 (d, J = 8.0 Hz, 2H), 7.65 (d, J =

8.0 Hz, 1H), 7.41 (d, J = 8.0 Hz, 2H), 7.34 (d, J = 16.0 Hz, 1H), 7.16 (d, J = 8.0 Hz, 1H), 6.87 (s, 1H), 6.74 (t, J = 8.0 Hz, 2H), 6.67 (s, 1H), 6.57 (s, 1H), 5.18 (s, 2H), 3.49-3.44 (m, J = 4H), 2.40 (t, J = 16.0 Hz, 4H), 1.75-1.65 (m, 2H), 1.12 (t, J = 8.0 Hz, 6H). ¹³C NMR (100 MHz, DMSO-d₆) δ 184.9, 160.6, 160.2, 158.6, 153.9, 153.1, 152.8, 148.3, 138.9, 137.2, 134.8, 132.6, 127.7, 127.0, 124.4, 120.8, 116.7, 115.4, 111.7, 110.6, 108.5, 101.6, 96.3, 70.1, 45.0, 44.9, 29.4, 25.0, 20.9, 12.8. MS (TOF): 604.4.

Compound CX-B-DF. Under N₂ atmosphere, compound **CX-B** (60 mg, 0.1 mmol) and MgSO₄ (1.0 g) was dissolved in CH₂Cl₂ (5 mL) and stirred for 0.5 h. And 5'-deoxy-5-fluorouridine (82 mg, 0.3 mmol) in DMF (5 mL) were added the above mixture. The reaction was refluxed for 12 h. Then, ice water (10 mL) was added, and the mixture was extracted with CH₂Cl₂/CH₃OH. The obtained organic layer dried by anhydrous Na₂SO₄ was filtered, and then the solvent was evaporated. The crude product was purified by the silica gel chromatography (CH₂Cl₂:CH₃OH = 5:1) to afford a blue solid. Yield: 28 mg (35%). ¹H NMR (400 MHz, DMSO-d₆) δ 11.89 (s, 1H), 8.52 (s, 1H), 8.10 (d, J = 4.0 Hz, 1H), 7.91 (d, J = 8.0 Hz, 1H), 7.81 (d, J = 8.0 Hz, 1H), 7.74 (d, J = 8.0 Hz, 1H), 7.64 (d, J = 8.0 Hz, 1H), 7.49 (d, J = 8.0 Hz, 1H), 7.41 (d, J = 8.0 Hz, 1H), 7.33 (d, J = 12.0 Hz, 1H), 7.15 (d, J = 8.0 Hz, 1H), 6.84 (d, J = 4.0 Hz, 1H), 6.73 (t, J = 8.0 Hz, 2H), 6.65 (s, 1H), 6.55 (s, 1H), 5.75 (s, 2H), 5.68 (d, J = 4.0 Hz, 1H), 4.09 (t, J = 8.0 Hz, 1H), 3.83 (t, J = 8.0 Hz, 1H), 3.70 (t, J = 8.0 Hz, 1H), 3.47-3.41 (m, 4H), 2.39 (t, J = 16.0 Hz, 4H), 1.43-1.35 (m, 2H), 1.27 (d, J = 4.0 Hz, 3H), 1.12 (t, J = 8.0 Hz, 6H). ¹³C NMR (100 MHz, DMSO-d₆) δ 184.8, 160.5, 160.0, 158.4, 157.6, 157.4, 153.8, 153.1, 152.8, 149.8, 149.5, 148.2, 141.7, 141.0, 139.4, 135.2, 134.7, 132.5, 127.3, 126.0, 125.6, 124.3, 120.8, 116.7, 115.5, 111.8, 110.5, 108.4, 101.5, 96.3, 91.8, 84.9,

82.5, 73.0, 44.9, 29.5, 25.1, 20.8, 19.0, 12.8. MS (TOF): 813.2. Elem. anal. (%) calcd. for $C_{45}H_{41}BFN_3O_{10}$: C, 66.43, H, 5.08, N, 5.16. Found: C, 66.31, H, 5.07, N, 5.18.

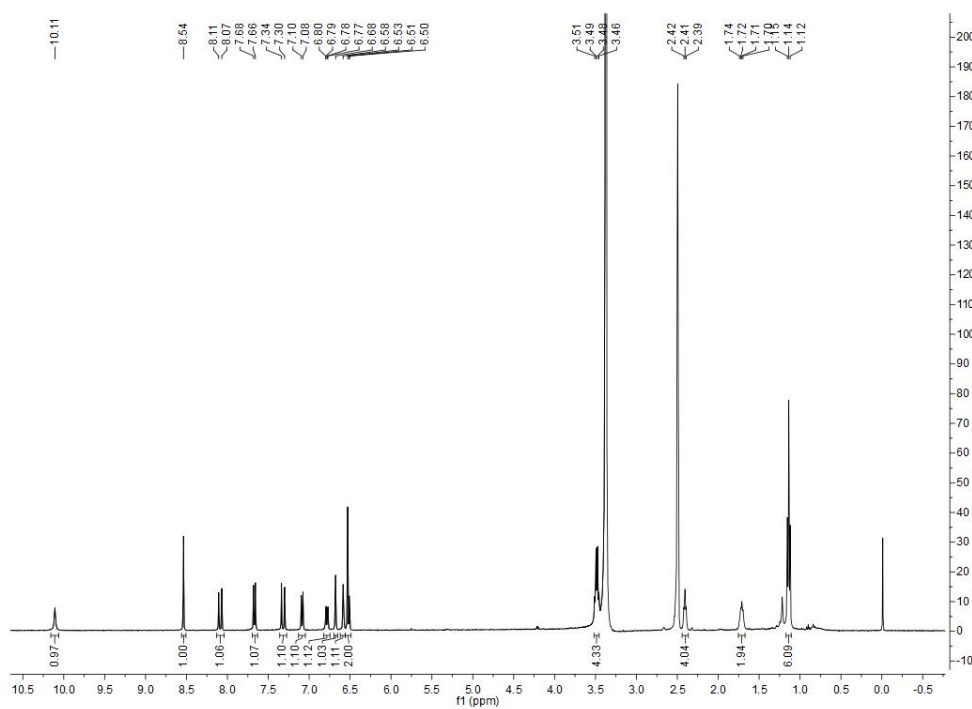


Fig. S1. 1H NMR spectra of CX-OH in DMSO- d_6 .

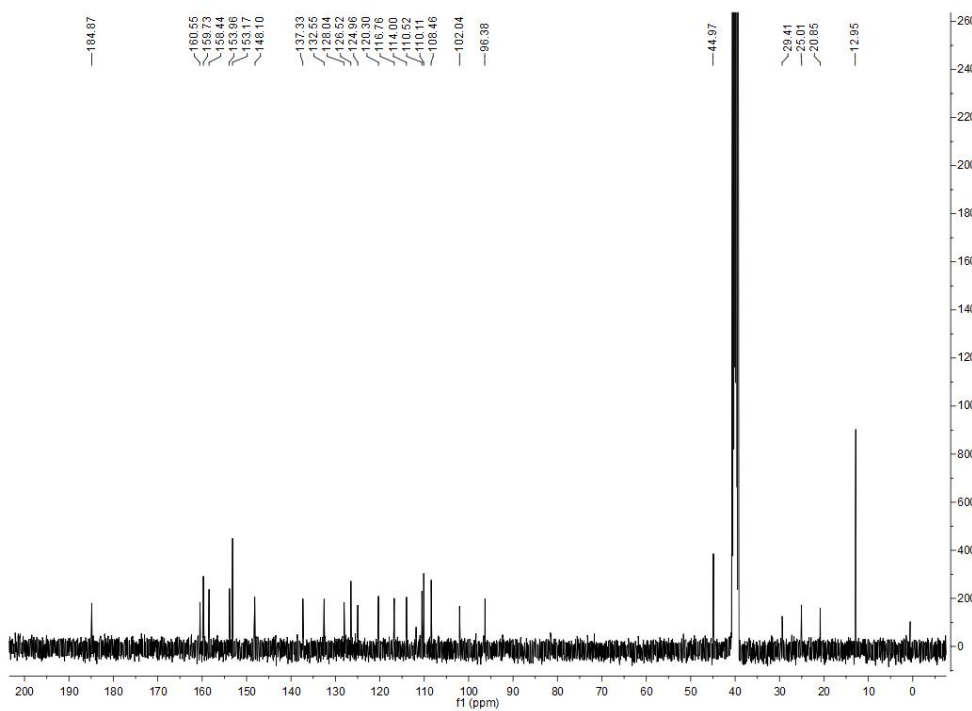


Fig. S2. ^{13}C NMR spectra of CX-OH in DMSO- d_6 .

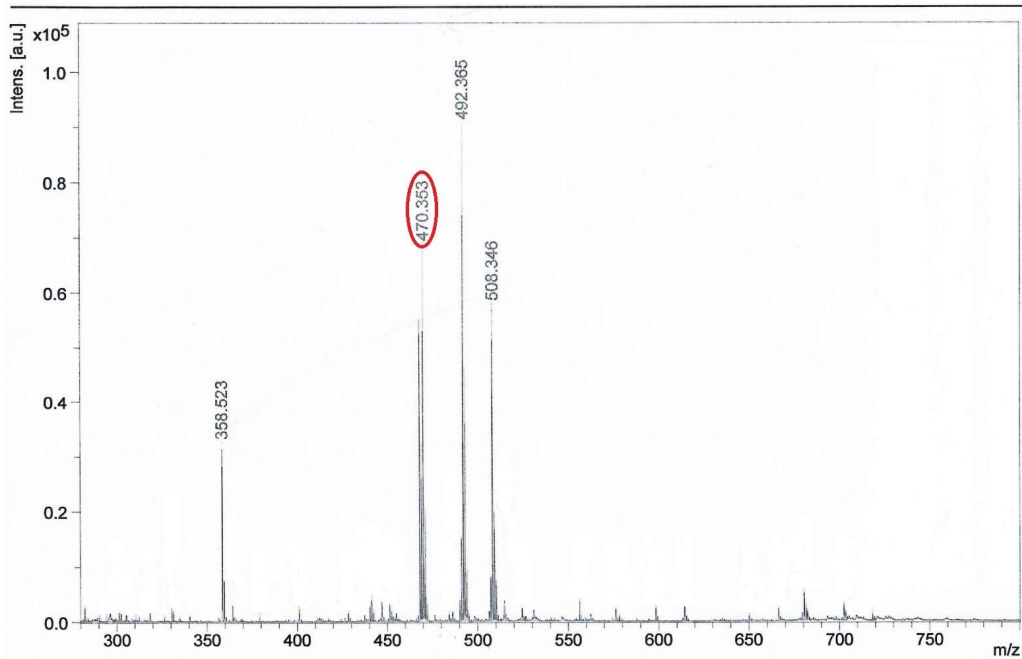


Fig. S3. Mass spectra of CX-OH.

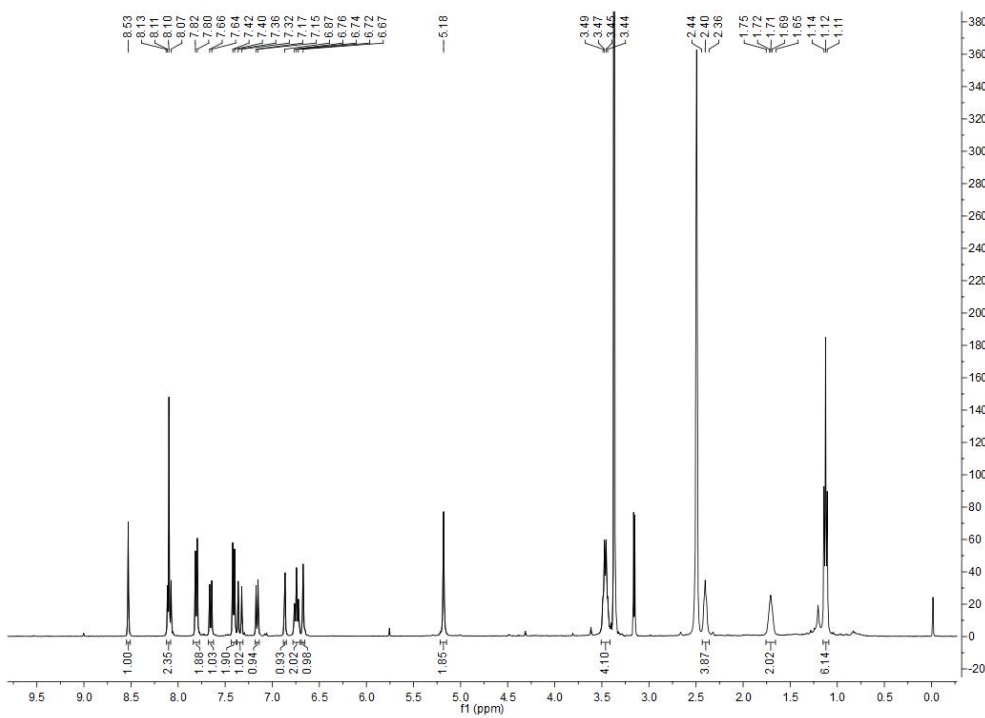


Fig. S4. ¹H NMR spectra of CX-B in DMSO-d₆.

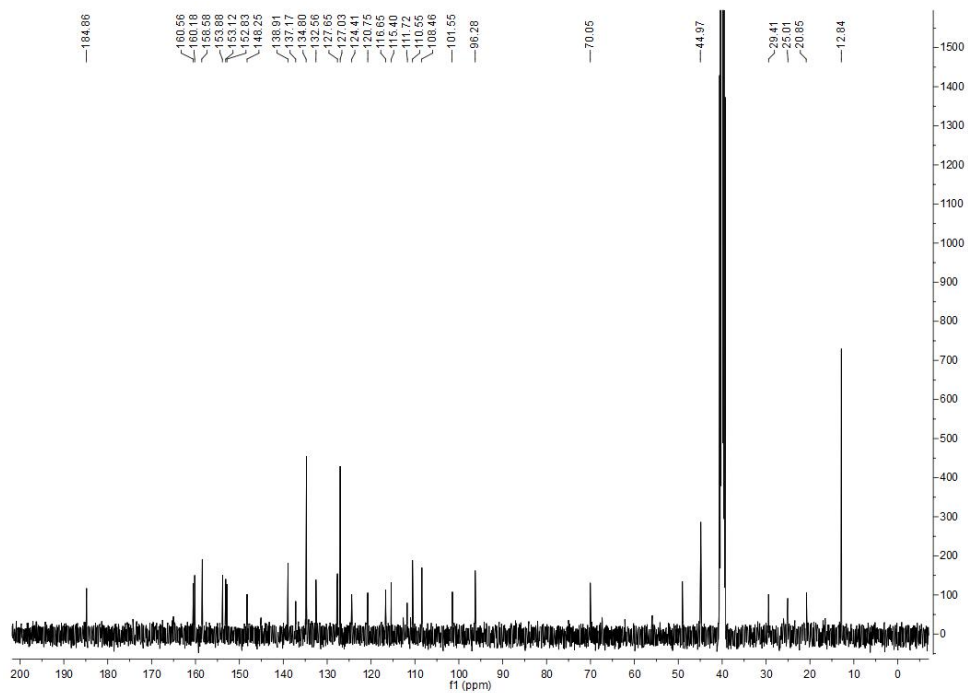


Fig. S5. ^{13}C NMR spectra of CX-B in DMSO-d_6 .

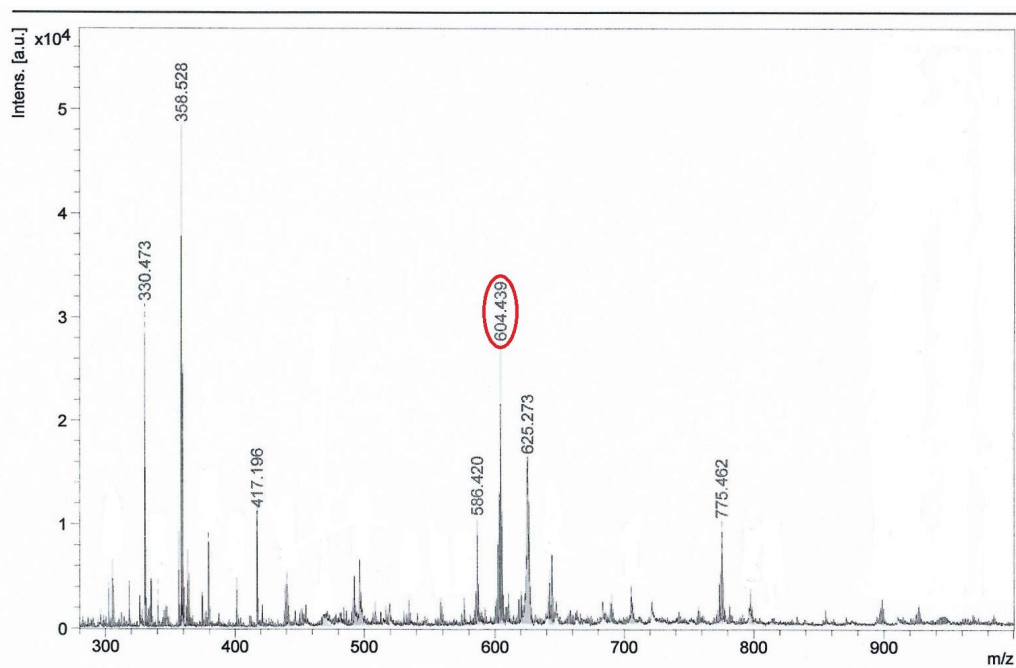


Fig. S6. Mass spectra of CX-B.

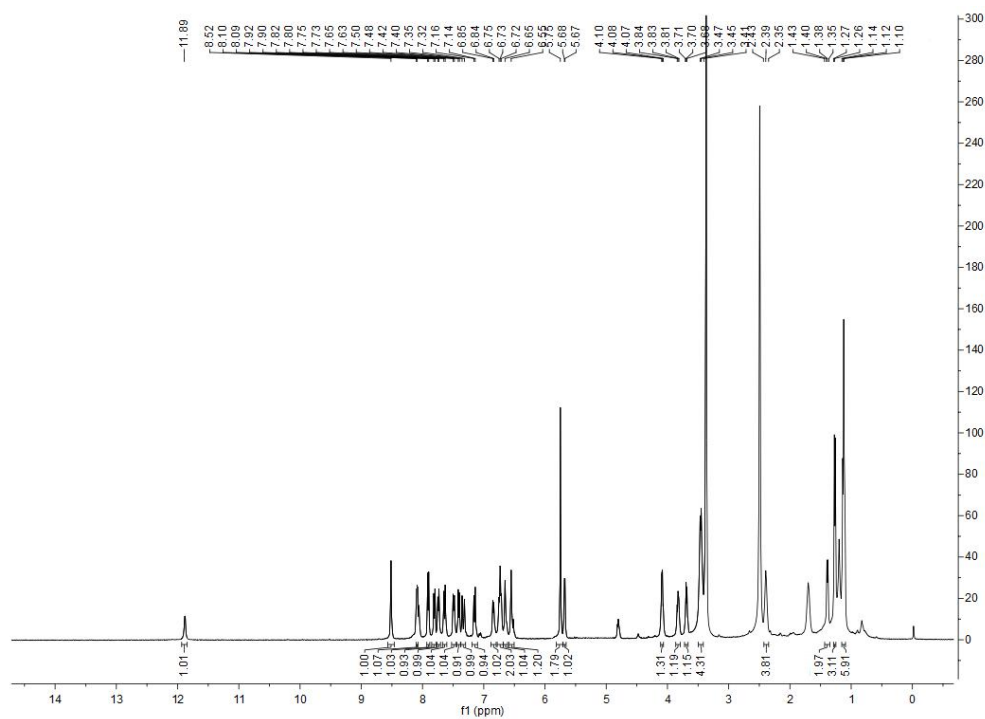


Fig. S7. ^1H NMR spectra of CX-B-DF in DMSO-d_6 .

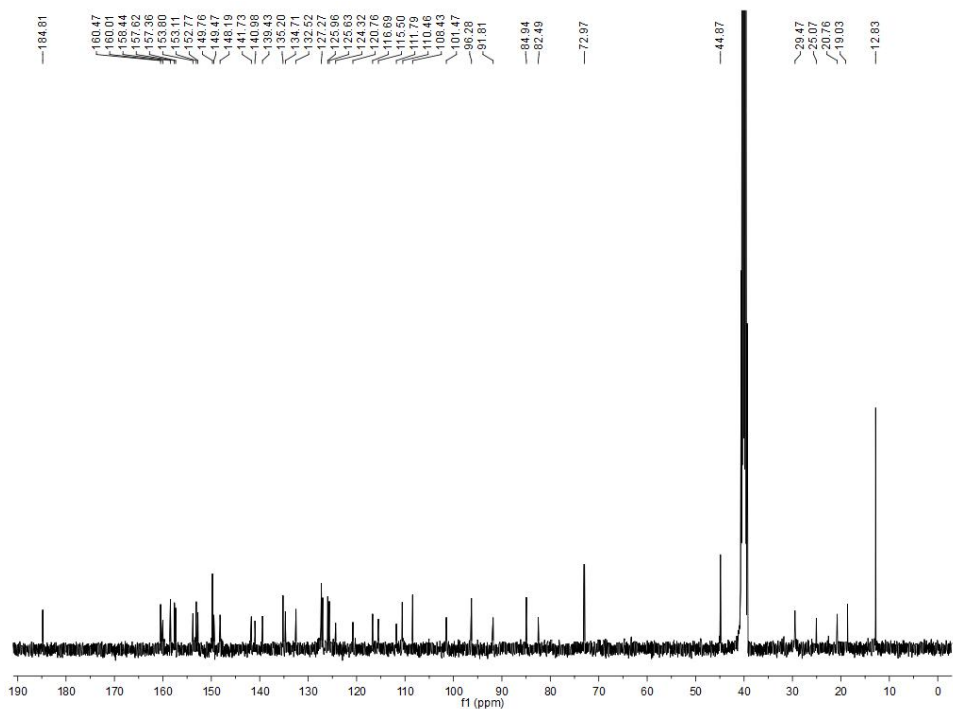


Fig. S8. ^{13}C NMR spectra of CX-B-DF in DMSO-d_6 .

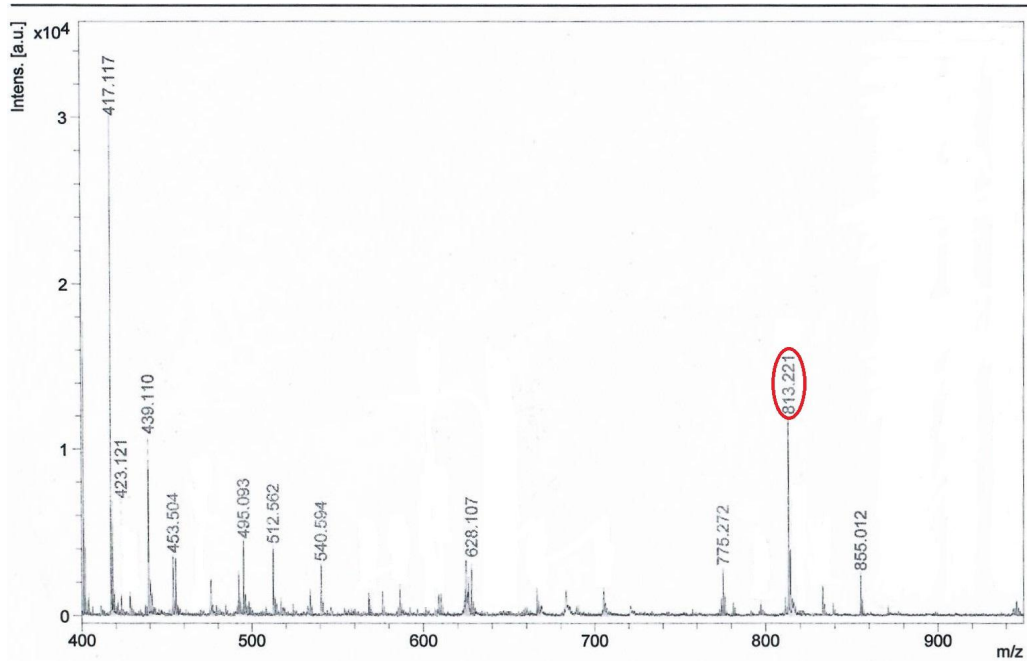


Fig. S9. Mass spectra of CX-B-DF.

3. Spectral data.

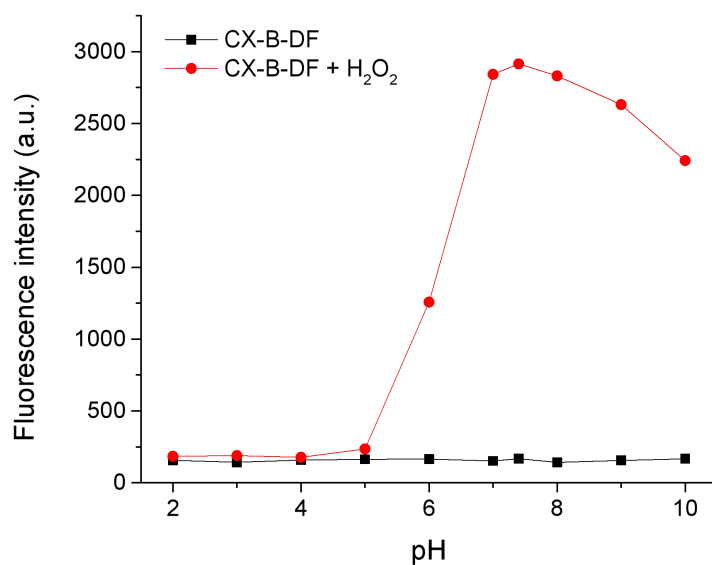


Fig. S10. Effect of pH on the fluorescence intensity of CX-B-DF (10 μM) before and after reaction with H_2O_2 (80 μM).

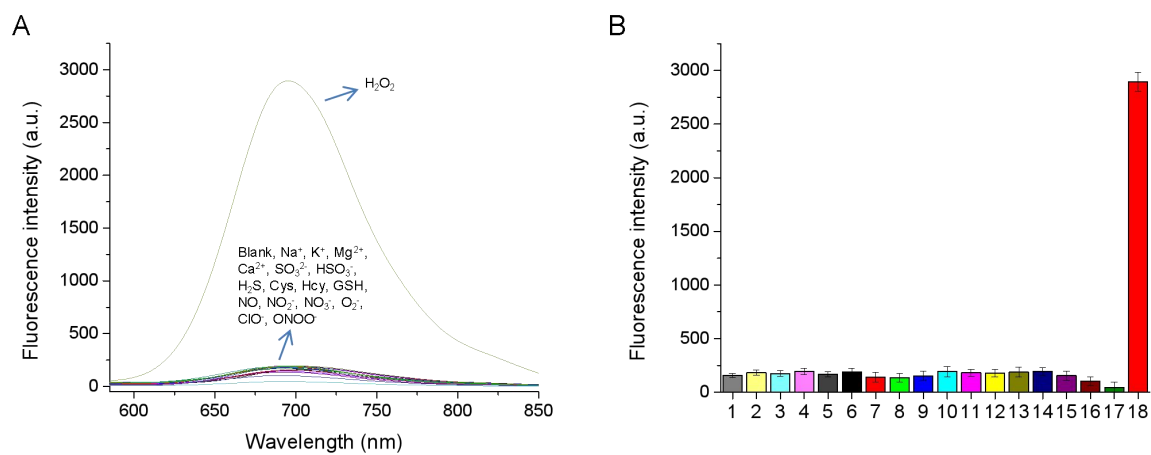


Fig. S11. Fluorescence spectra of CX-B-DF (10 μM) toward different analytes (200 μM): 1. blank; 2. Na⁺; 3. K⁺; 4. Mg²⁺; 5. Ca²⁺; 6. SO₃²⁻; 7. HSO₃⁻; 8. H₂S; 9. Cys; 10. Hcy; 11. GSH; 12. NO; 13. NO₂⁻; 14. NO₃⁻; 15. O₂⁻; 16. ClO⁻; 17. ONOO⁻; 18. H₂O₂.

4. Response mechanism.

On the basis of the above spectral data, a possible response mechanism of CX-B-DF to H_2O_2 is proposed. The prodrug itself is non-fluorescent due to the protection of hydroxyl group by the borate ester. After adding H_2O_2 , the hydroxyl group of the probe is exposed and 5'-DFUR is released, resulting in the recovery of the intramolecular charge transfer (ICT) process and the appearance of a strong fluorescence signal.

To prove the speculation, HPLC experiments were carried out (Fig. S12). The retention time of CX-B-DF itself is 2.9 min. After adding H_2O_2 , the signal peak of CX-B-DF declines and a new peak appears at 6.1 min (the same retention time with fluorophore CX-OH). Moreover, MS analysis was also investigated. For CX-B-DF, the peak is at $m/z = 813.2$. When CX-B-DF reacts with H_2O_2 , the peak at $m/z = 813.2$ reduces and the new peaks of CX-OH and 5'-DFUR are found at m/z 470.3 and 244.2, respectively (Fig. S13). The above results show that CX-B-DF can be effectively cleaved by H_2O_2 and then release free fluorophore (CX-OH) and inactive drug (5'-DFUR).

At the same time, we performed the density functional theory (DFT) calculation by using Gaussian 09 package. The optimized structures of CX-B-DF and CX-OH were shown in Fig. S14A. And their frontier molecular orbitals were given in Fig. S14B. These results show that CX-OH is composed of a donor and an acceptor, making the ICT process constitute a push-pull system and causing the fluorescence turn on. In contrast, the borate ester group in CX-B-DF hinders the ICT process, causing the fluorescence turn-off. The theoretical calculation is consistent with the experimental results, verifying the fluorescence change of the probe is due to the reaction between CX-B-DF and H_2O_2 .

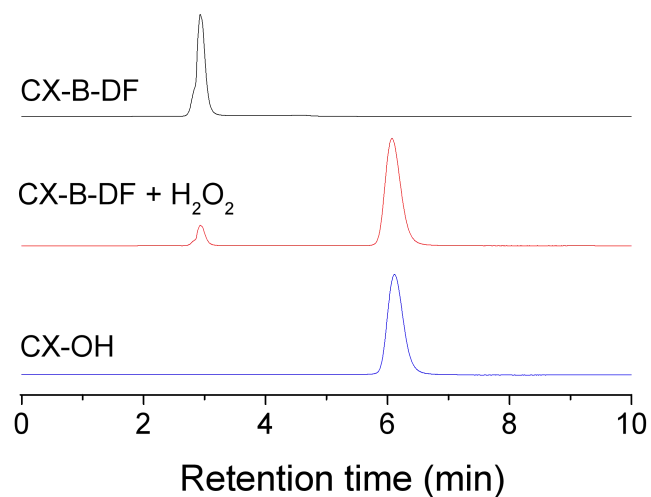


Fig. S12. HPLC chromatograms of CX-B-DF, CX-B-DF reacted with H₂O₂ and CX-OH.

HPLC mobile phase: methanol/H₂O = 95/5 (v/v).

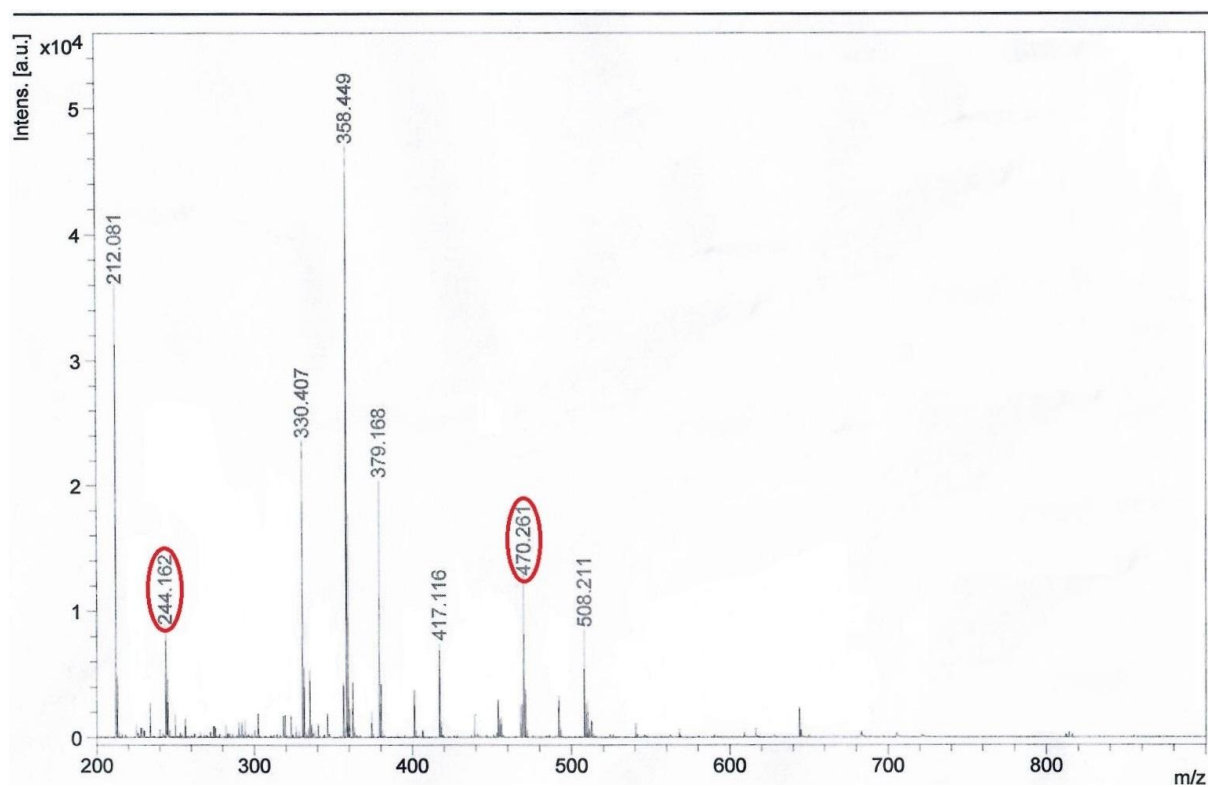


Fig. S13. Mass spectra of CX-B-DF with H₂O₂.

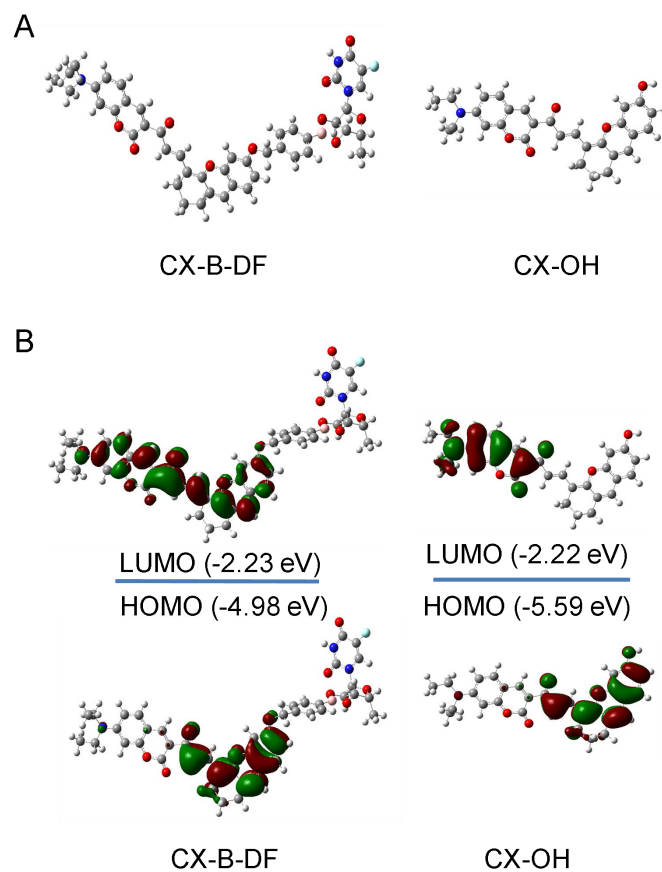


Fig. S14. (A) The optimized structures of CX-B-DF and CX-OH. In the ball-and-stick model, carbon, oxygen and nitrogen atoms are colored in gray, red and blue, respectively. (B) Frontier molecular orbitals of CX-B-DF and CX-OH.

5. Biological assays.

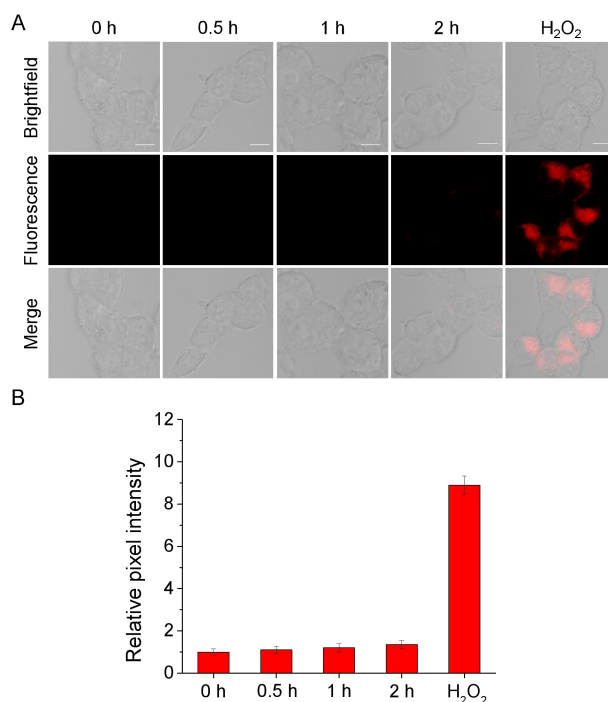


Fig. S15. (A) Fluorescence imaging of H₂O₂ in 293T cells. The cells were incubated with CX-B-DF (10 μ M) for 0 h, 0.5 h, 1 h and 2 h, respectively, or the cells were pretreated with H₂O₂ (50 μ M) for 0.5 h and then incubated with CX-B-DF for 0.5 h. (B) Relative pixel intensity. $\lambda_{\text{ex}} = 560 \text{ nm}$, $\lambda_{\text{em}} = 650\text{-}750 \text{ nm}$; Scale bar:10 μm .

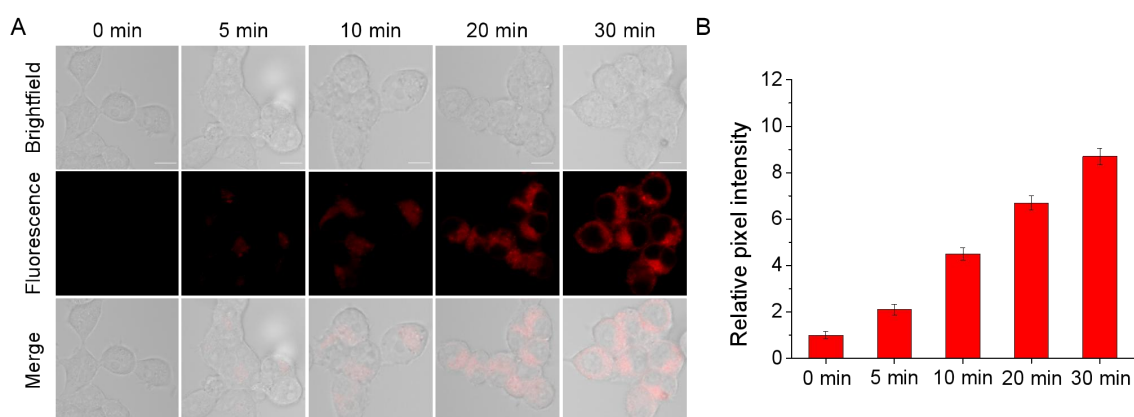


Fig. S16. Fluorescence imaging of H₂O₂ in 293T cells. The cells were incubated with H₂O₂ (50 μ M) for 0.5 h and then incubated with CX-B-DF for 0-30 min. $\lambda_{\text{ex}} = 560 \text{ nm}$, $\lambda_{\text{em}} = 650\text{-}750 \text{ nm}$; Scale bar:10 μm .

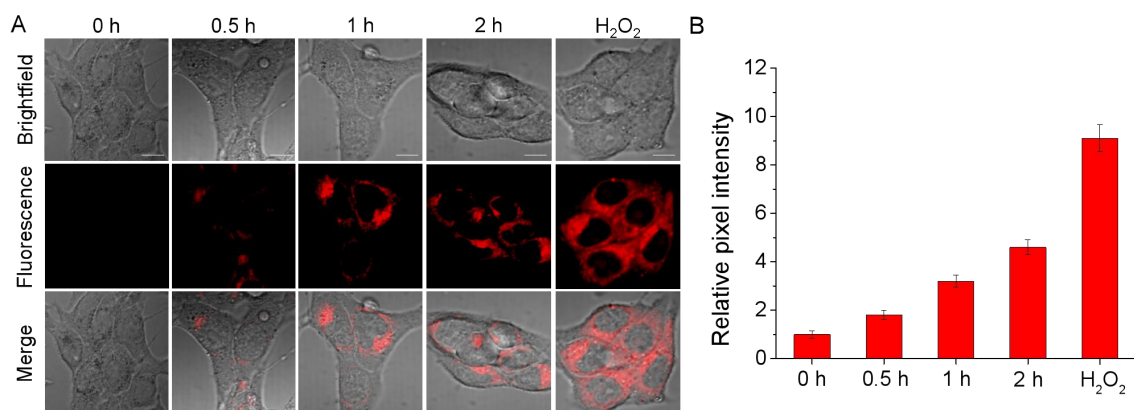


Fig. S17. (A) Fluorescence imaging of H₂O₂ in 4T1 cells. The cells were incubated with CX-B-DF (10 μM) for 0 h, 0.5 h, 1 h and 2 h, respectively, or the cells were pretreated with H₂O₂ (50 μM) for 0.5 h and then incubated with CX-B-DF for 0.5 h. (B) Relative pixel intensity. $\lambda_{\text{ex}} = 560 \text{ nm}$, $\lambda_{\text{em}} = 650\text{-}750 \text{ nm}$; Scale bar: 10 μm.

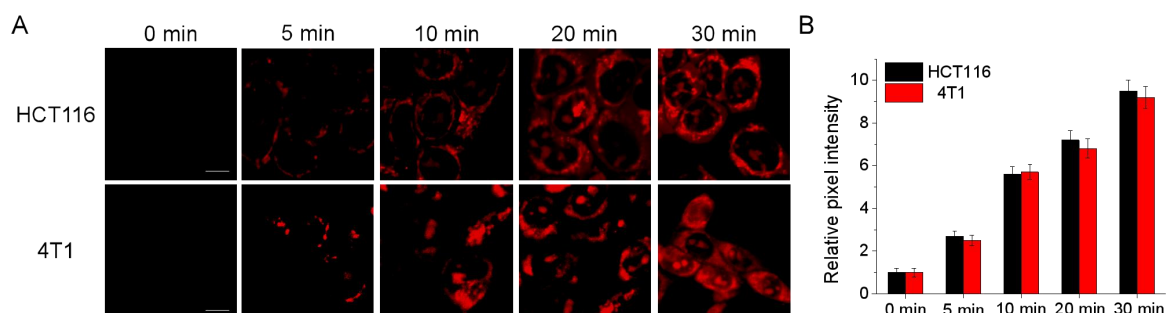


Fig. S18. Fluorescence imaging of H₂O₂ in HCT116 and 4T1 cells. The cells were incubated with H₂O₂ (50 μM) for 0.5 h and then incubated with CX-B-DF for 0-30 min. $\lambda_{\text{ex}} = 560 \text{ nm}$, $\lambda_{\text{em}} = 650\text{-}750 \text{ nm}$; Scale bar: 10 μm.

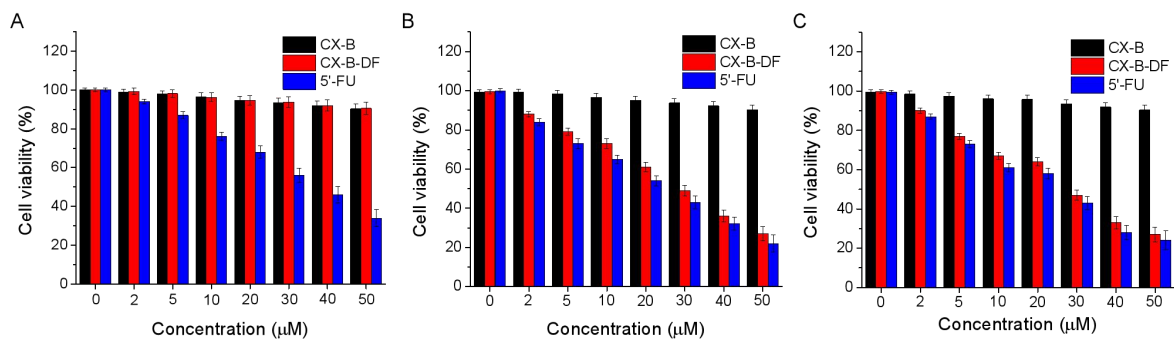


Fig. S19. CCK-8 assay for estimating cell viability (%) of (A) 293T cells, (B) 4T1 cells and (C) HCT116 cells treated with various concentrations of CX-B, CX-B-DF and 5'-FU after 24 h incubation.

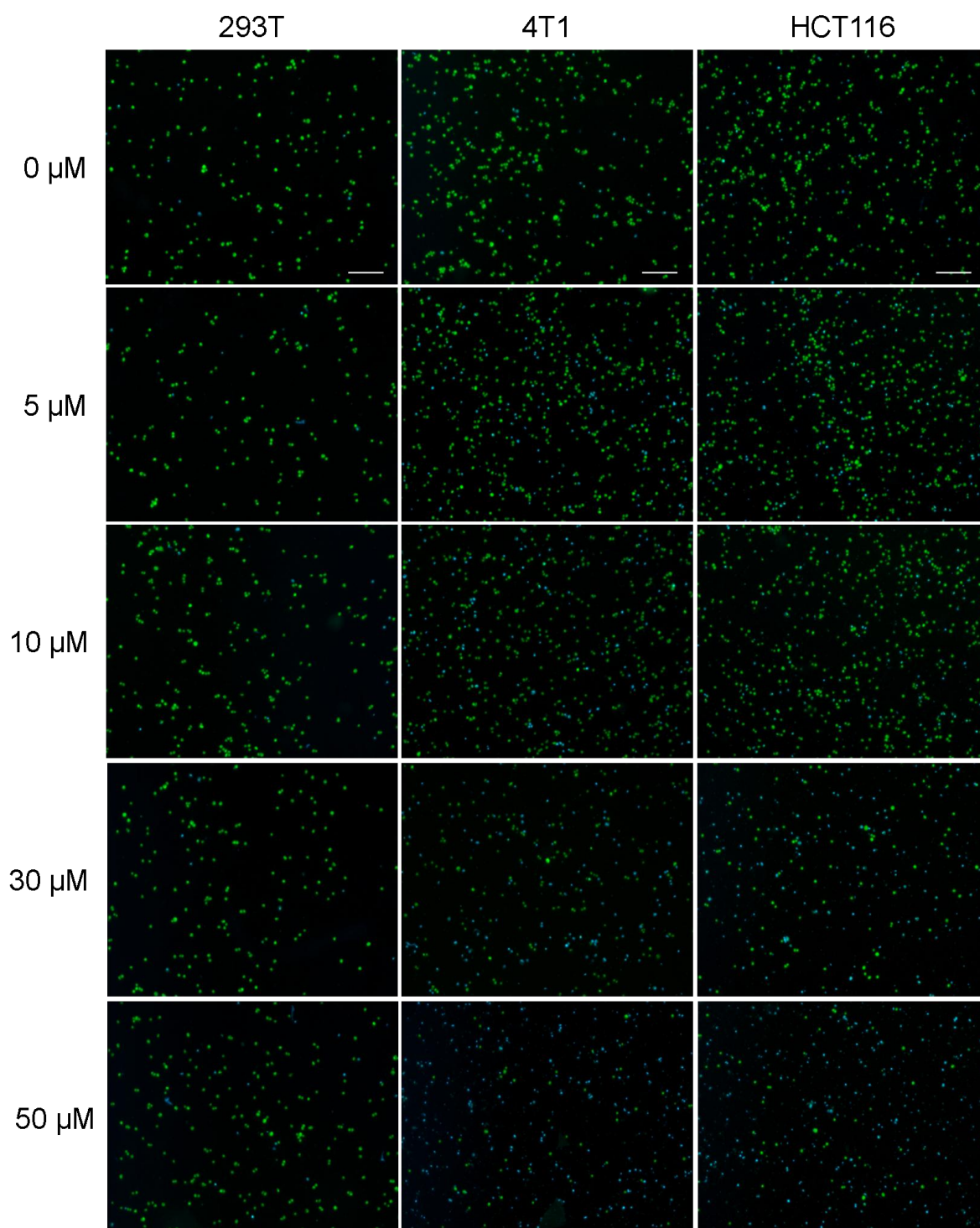


Fig. S20. AO/DAPI staining for estimating cell viability (%) of 293T cells, 4T1 cells and HCT116 cells treated with various concentrations of CX-B-DF (0, 5, 10, 30, 50 μM) after 24 h incubation. All the cells were stained by AO with green fluorescence, whereas dead cells were stained by DAPI with blue fluorescence. Scale bar: 100 μm .

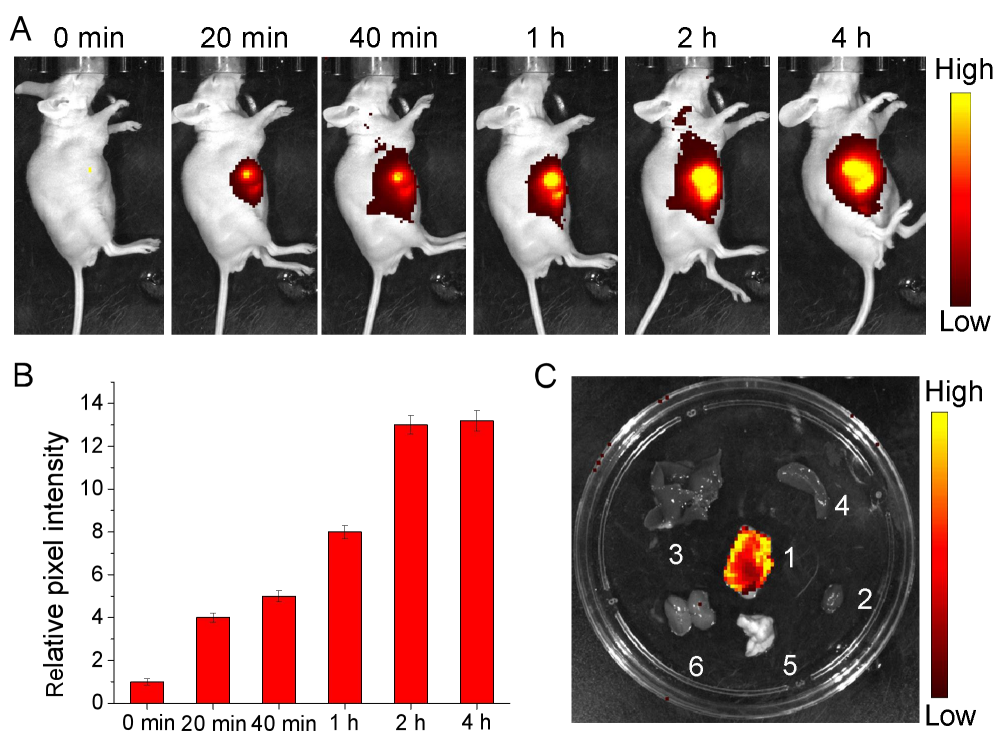


Fig. S21. (A) Fluorescence imaging of tumor-bearing mice after intratumoral injection of CX-B-DF (200 μ M) with time (0 min, 20 min, 40 min, 1 h, 2 h, 4 h). (B) Relative pixel intensity in (A). (C) Fluorescence imaging of tumor and main organs. 1: tumor, 2: heart, 3: liver, 4: spleen, 5: lungs, 6: kidney. $\lambda_{\text{ex}} = 560 \text{ nm}$, $\lambda_{\text{em}} = 650\text{-}750 \text{ nm}$.

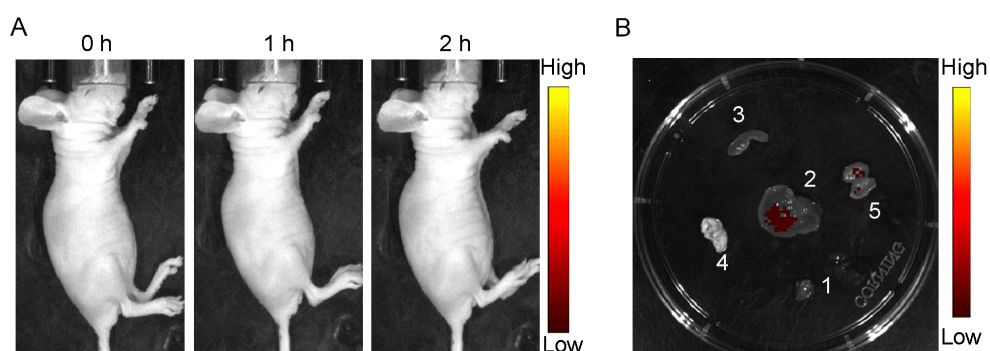


Fig. S22. (A) Fluorescence imaging of normal mice after intravenous injection of CX-B-DF (200 μ M) with time (0 h, 1 h, 2 h). (B) Fluorescence imaging of tumor and main organs. 1: heart, 2: liver, 3: spleen, 4: lungs, 5: kidney. $\lambda_{\text{ex}} = 560 \text{ nm}$, $\lambda_{\text{em}} = 650\text{-}750 \text{ nm}$.

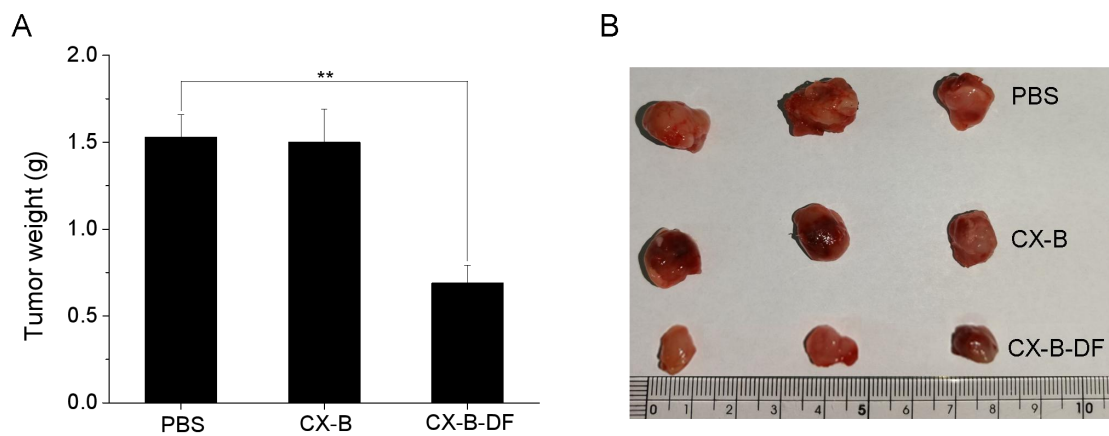


Fig. S23. (A) Average tumor weight after treatments with (PBS, CX-B, CX-B-DF). (n = 3, data expressed as average \pm SE, * and ** means $P < 0.05$, or < 0.01 , respectively). (B) The photograph of tumors.